Electrical Power and Energy Systems 146 (2023) 108737

Contents lists available at ScienceDirect

International Journal of Electrical Power and Energy Systems

journal homepage: www.elsevier.com/locate/ijepes

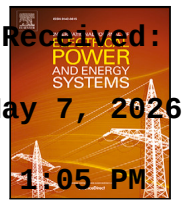

Evaluating grid strength under uncertain renewable generation

Manisha Maharjan [a,b,*], Almir Ekic [a], Mari Beedle [a], Jin Tan [c], Di Wu [a]

[a] Department of Electrical and Computer Engineering, North Dakota State University (NDSU), 1411 Centennial Blvd, Fargo, 58105, ND, USA
[b] Electricity Infrastructure and Buildings Division, Pacific Northwest National Laboratory (PNNL), 1902 Battelle Blvd, Richland, 99352, WA, USA
[c] Power Systems Engineering Center, National Renewable Energy Laboratory (NREL), 15013 Denver W Pkwy, Golden, 80401, CO, USA

ARTICLE INFO

MSC:
0000
1111

Keywords:
Grid strength
Probabilistic collocation method
Uncertainty analysis
Renewable energy resources

ABSTRACT

The increasing displacement of synchronous generators with renewable resources such as wind and solar via power electronic interfaces causes a reduction in short-circuit strength and weak grid issues. The variation and uncertainty of renewable energy increase challenges for identifying weak grid conditions. This paper proposes an efficient method to analyze the impact of uncertain renewable energy on grid strength. The proposed method uses the probabilistic collocation method (PCM) to approximate the results of grid strength assessment under uncertain renewable generation, in order to reduce computational burden without compromising result accuracy when compared with traditional Monte Carlo simulation (MCS). To improve the accuracy of the approximation results, the proposed method integrates the K-means clustering technique with PCM to select the approximation samples of input variables. The efficacy of the proposed method is demonstrated by comparison with MCS on the modified IEEE 9-bus system and modified IEEE 39-bus system with multiple renewable generators.

1. Introduction

Integration of inverter-based renewable energy resources (IB-RERs) like wind and solar in North American power grid has surpassed 100 GW in 2016 [1]. While the IB-RERs supply clean energy to electricity customers, they pose many challenges in grid planning and operation. The IB-RERs provide expected real and reactive power based on the electronic controls, which separate the power source from the grid. The predominant control strategy for contemporary IB-RERs is grid-following, where a phase-locked loop tracks the voltage at the point of interconnection (POI), which is, in general, assumed to be stiff [1], with which an output current is generated to achieve power set points. An associated challenge with high instantaneous penetrations of grid-following IB-RERs is the reduction of synchronous generation that forms the basis of this stiff grid assumption, which results in a weak grid. Under weak grid conditions, the grid voltage is sensitive to active and reactive power disturbances, which may result in potential voltage stability and grid reliability issues. Such weak grid issues are becoming prominent due to the variability and uncertainty of renewable generation [2].

Potential weak grid issues are usually analyzed and identified based on grid strength assessment. In the assessment, short-circuit ratio (SCR) is an index recommended by North American Electric Reliability Corporation (NERC) to quantify the grid strength [1,3]. The commonly used SCR calculation method ignores the interactions among IB-RERs and thus may cause an inaccurate estimation of grid strength at POIs for IB-RERs [1,4]. To consider the effect of IB-RERs interactions on grid strength, several new methods have been developed, such as the weighted short-circuit ratio (WSCR) method developed by the Electric Reliability Council of Texas (ERCOT) [4] and the composite short-circuit ratio (CSCR) method developed by GE Energy Consulting [5]. Both CSCR and WSCR methods do not consider the real electrical network connections among IB-RERs, and therefore do not reflect the actual strength of the grid at the POIs. Moreover, both these methods mainly provide the aggregated strength of a power grid in the area where the IB-RERs are interconnected electrically close, but they do not calculate the strength of the grid at each individual POI in the specific area. To overcome those shortcomings, various metrics have been proposed, such as the site-dependent short-circuit ratio (SDSCR) method is proposed in [6], network response short-circuit ratio (NRSCR) [7], generalized short-circuit ratio (gSCR) [8], and hybrid multi-infeed effective short-circuit ratio (HMIESCR) [9]. The gSCR and HMIESCR are proposed for grid strength analysis in multi-infeed HVDC (MIDC) systems, while the SDSCR and NRSCR are mainly proposed for grid strength assessment in power systems with high penetration of renewable resources. In addition, the SDSCR has further been extended to

* Corresponding author at: Department of Electrical and Computer Engineering, North Dakota State University (NDSU), 1411 Centennial Blvd, Fargo, 58105, ND, USA.
E-mail address: manisha.maharjan@pnnl.gov (M. Maharjan).

https://doi.org/10.1016/j.ijepes.2022.108737
Received 16 June 2022; Received in revised form 14 September 2022; Accepted 18 October 2022
Available online 18 November 2022

effective site-dependent short circuit ratio (ESDSCR), which considers the impact of interconnected capacitors at POIs on grid strength in power systems with high penetration of renewable resources [10].

With the intermittent nature of renewable generation resulting from uncertain weather conditions, grid strength may change with uncertain renewable generation. Thus, quantifying the impact of uncertain renewable generation on grid strength will be critical to prevent the potential weak grid issues via grid planning and operation, especially in an IB-RER-dominated grid. Traditionally, the uncertainty evaluation can be evaluated using Monte Carlo simulation (MCS) [11–13]. However, the MCS typically repeats deterministic grid strength analysis by using a massive number of renewable generation samples to render the uncertainty characteristics of the results.

To improve simulation efficiency, this paper proposes an uncertainty evaluation algorithm to quantify the impact of uncertain renewable generation on grid strength based on the probabilistic collocation method (PCM). The PCM has been studied for uncertainty analysis in numerous power system studies [14–18]. The proposed algorithm can use the probability distributions of renewable generation to quantify the probabilistic characteristics of grid strength through a set of orthogonal polynomials to approximate the original models. The calculation is made to determine the parameters in the approximation functions which can obtain the desired precision of results using a small number of simulations. Therefore, the proposed algorithm significantly reduces the computational burden and outperforms MCS thousands of times in terms of simulation efficiency. To further enhance the accuracy of the proposed algorithm, the K-means clustering technique is introduced to the PCM for selecting the representative approximation samples to describe the probabilistic characteristics of uncertain renewable generation. The major contributions of this paper are summarized as follows.

(1) An uncertainty evaluation algorithm is proposed to quantify the impact of uncertain renewable generation on grid strength by integrating the PCM with grid strength assessment. Since the PCM can obtain accurate results using a small set of simulations, this method can potentially be used to save computational cost without compromising the result accuracy compared to the MCS simulation.

(3) The K-means clustering technique is introduced to the PCM to select the representative approximation samples for improving the approximation accuracy for grid strength analysis under uncertain renewable generation.

(3) The efficacy of the proposed algorithm is validated on the modified IEEE 9-bus and IEEE 39-bus systems.

The rest of this paper is organized as follows. In Section 2, grid strength assessment is discussed. In Section 3, the principle of PCM is introduced. Section 4 presents our proposed method for quantifying the impact of uncertain renewable generation on grid strength. The efficacy of the proposed method is demonstrated in Section 5. In Section 6, the conclusions are drawn.

2. Grid strength assessment

Grid strength assessment can help grid engineers identify and understand "weak" grid issues for reliably planning and operating the power grid. Grid strength is a measure of an electrical power system that evaluates the change in voltage and operating conditions, following a disturbance in the power system [19]. The strength of a power grid at POI is commonly quantified by SCR, which is the ratio of the short circuit capacity at the POI to the rated capacity or injected power from the IB-RER. A power grid with lower SCR value is susceptible to voltage instability, therefore known as weak grid. However, SCR does not include the effect of the reactive power compensation from the shunt capacitor at the buses for measuring the grid strength and therefore can underestimate grid strength. To account for the impact, the grid strength is calculated using effective short circuit ratio (ESCR), which is defined as [20],

$$ESCR_i = \frac{|S_{ac,i} - jQ_{c,i}|}{P_{R,i}} \tag{1}$$

where symbol |.| indicates the magnitude of a complex quantity; $S_{ac,i} = |V_{R,i}|^2/|Z_{R,i}|$ is the short-circuit capacity of the grid at POI i; $V_{R,i}$ is the voltage at POI i; $Z_{R,i}$ is the Thevenin equivalent impedance seen at POI i; $P_{R,i}$ is the rated capacity or injected power from the IB-RER at POI i $Q_{c,i} = |V_{R,i}|^2/|X_c|$ is the reactive compensation from shunt with shunt capacitive reactance X_c at POI i.

ESCR defined in (1) considers the impact of the reactive power compensation from shunt capacitor at POI on grid strength, it cannot account for the interactions among the capacitors and the interactions among multiple IB-RERs in a power grid. Especially, when IB-RERs are electrically close, the interactions have significant impacts on the strength of their POIs. To include these impacts for grid strength assessment, the effective site-dependent SCR (ESDSCR) was proposed in [10],

$$ESDSCR_i = \frac{|S_{ac,i} - jQ_{ceq,i}|}{P_{Req,i}} = \frac{|S_{ac,i} - jQ_{c,i} - \sum_{j\epsilon R, j\neq i} \alpha_{ij} jQ_{c,j}|}{(|P_{R,i} + \sum_{j\epsilon R, j\neq i} \beta_{ij} P_{R,j}|)} \tag{2}$$

$$\alpha_{ij} = \frac{Z_{RR,ij}}{Z_{RR,ii}} \cdot \left(\frac{V_{R,j}}{V_{R,i}}\right), \qquad \beta_{ij} = \frac{Z_{RR,ij}}{Z_{RR,ii}} \cdot \left(\frac{V_{R,i}}{V_{R,j}}\right)^* \tag{3}$$

where **R** is the set of all POIs connected to IB-RERs; $Z_{RR,ij}$ is the (ith, jth) element in the submatrix of bus impedance matrix that is only related to buses connected to IB-RERs; and symbol * indicates the complex conjugate of a complex quantity.

The ESDSCR defined in (2) considers the impact of the interactions among IB-RERs and capacitors on the grid strength at POI i by interaction factors α_{ij} and β_{ij}. The ESDSCR at bus i accounts for the reactive compensation from the shunt capacitor connected at bus i ($Q_{c,i}$) and the reactive compensation from other capacitors in different locations ($Q_{c,j}$) using the interaction factor α_{ij} as defined in (3). Moreover, ESDSCR at bus i utilizes the real power injected by the IB-RER directly connected to bus i ($P_{R,i}$) and the real power injection from other IB-RERs at different locations in the power grid ($P_{Req,i}$), scaled by the interaction factor β_{ij} as defined in (3). The ESCR in (1) can be considered as a special case of the ESDSCR when only one shunt element is connected to one IB-RER in the power grid in (1). Thus, the ranges of ESCR for grid strength evaluation is also relevant to ESDSCR. For instance, if the ESDSCR value is larger than 3 ($ESDSCR > 3$), then the power grid is strong at a POI ; if ESDSCR value is between 2 and 3 ($2 < ESDSCR < 3$), the grid is weak at a POI; and if ESDSCR value is smaller than 2 ($ESDSCR < 2$), the grid is very weak at a POI.

From (2), it can be seen that the ESDSCR is related to renewable generation $P_{R,i}$ at different POIs. The intermittent characteristics of renewable energy under uncertain weather conditions may have a detrimental impact on grid strength, and this impact could be aggravated with the increase in the penetration level of renewable energy. Under variable renewable generation, evaluating grid strength based on the ESDSCR may consider all feasible uncertain scenarios, which is computational daunting. To address the challenge, this paper proposes a probabilistic approach by integrating the PCM with the ESDSCR-based method to reduce computational cost compared with the straightforward application of MCS.

3. Probability collocation method (PCM)

PCM is an uncertainty modeling approach using Gaussian quadrature to map the relationship between the uncertain input parameters and the output. In the PCM, the relationship between the uncertain parameter and the output response is represented through polynomial equation to identify a good set of simulations for correctly and robustly determining the mapping. The PCM model is derived based on the concept of orthogonal polynomials [15].

3.1. Orthogonal polynomials

Two polynomial functions $H_1(x)$ and $H_2(x)$ are orthogonal only if their inner product is zero [21]. The inner product of $H_1(x)$ and $H_2(x)$ is calculated using,

$$\langle H_1(x), H_2(x)\rangle = \int_{\mathfrak{R}} f(x)H_1(x)H_2(x)dx \tag{4}$$

where $f(x)$ is any non-negative weighting function defined in a space $\mathfrak{R}$. A set of orthogonal polynomial functions $H_1(x)$, $H_1(x)$, …, $H_n(x)$ can be defined as a polynomial family of orthogonal polynomials, if they satisfy the following condition,

$$\left\langle H_i(x), H_j(x)\right\rangle = \begin{cases} 1, i = j \\ 0, i \neq j \end{cases} \tag{5}$$

where $H_i(x)$ is the ith order of the polynomial function. For each order i, $H_i(x)$ has exactly i roots within the space of $\mathfrak{R}$. These roots are termed as collocation points which are used to evaluate the coefficients of the approximation model $\hat{g}(x)$. The $(-1)^{th}$ and 0th order polynomials are defined to be 0 and 1, respectively.

$$\begin{aligned} H_{-1}(x) &= 0 \\ H_0(x) &= 1 \end{aligned} \tag{6}$$

Gaussian quadrature integration in (4) approximates the numeric value for the integral by selecting appropriate x values to evaluate $g(x)$ and calculate the integral [14],

$$\int_{\mathfrak{R}} f(x)g(x)h(x)dx \approx \sum_{i=1}^{n} f_i g(x_i) \tag{7}$$

where f_i is the coefficient determined by the weighting function $f(x)$, and $g(x_i)$ is computed based on x_i, which are the roots of the higher orthogonal polynomials.

3.2. PCM-based approximation

3.2.1. Approximation model for a single input variable

For a single uncertain parameter x with its probability density function (pdf) $f(x)$, the estimated output is a function of the input uncertain parameter x. The estimated output is represented by $\hat{g}(x)$ in polynomial form as,

$$\hat{g}(x) = k_0H_0(x) + k_1H_1(x)+...+k_{n-1}H_{n-1}(x) \tag{8}$$

where k_i is constant coefficient, $H_i(x)$ is orthogonal polynomial of uncertain input x, and n is the order of the PCM model.

The coefficients k_i can be solved by the following equation with n samples $(x_i, \hat{g}(x_i))$ from the original function $\hat{g}(x)$,

$$\begin{bmatrix} k_{n-1} \\ \vdots \\ k_0 \end{bmatrix} = \begin{bmatrix} H_{n-1}(x_1) & \cdots & H_0(x_1) \\ \vdots & \ddots & \vdots \\ H_{n-1}(x_n) & \cdots & H_0(x_n) \end{bmatrix}^{-1} \begin{bmatrix} \hat{g}(x_1) \\ \vdots \\ \hat{g}(x_n) \end{bmatrix} \tag{9}$$

where x_1, …, x_n are the collocation points, $\hat{g}(x_1)$, …, $\hat{g}(x_n)$ are the responses of the output at the collocation points, and $H_0(x)$, …, $H_{n-1}(x)$ are the orthogonal polynomials calculated at the collocation points. These coefficients are replaced in (8) to obtain the PCM approximate model. The statistics of the output response for a given range of the uncertain input parameter can be calculated simply using these coefficients. The expected value of output is $\mu[\hat{g}(x)] = k_0$ and the variance of the output value is $\sigma^2[\hat{g}(x)] = \sum_{i=1}^{n-1} {k_i}^2$.

3.2.2. Approximation model for multiple input variables

For multiple uncertain parameters x_1, x_2, …, x_n with independent pdfs $f(x_1)$, $f(x_2)$,…, $f(x_n)$, the approximation model can be estimated using,

$$\hat{g}(x) = k_0+\sum_{i=1}^{n}[k_{i1}H_{i1}(x_i)+\cdots+k_{im}H_{im}(x_i)]+\sum_{i=1}^{n}\sum_{\substack{j=1 \\ j\neq i}}^{n}[k_iH_{i1}(x_i)H_{j1}(x_j)] \tag{10}$$

where k_0, k_{i1}, …, k_{im} are the coefficients, and $H_{i1}(x_i)$, …, $H_{im}(x_i)$ are orthogonal polynomials for uncertain parameter x_i [16]. The model coefficients can be determined by using the collocation points similar to that of single uncertain parameter. However, the number of collocation points for single uncertain parameter is (m+1) for mth order PCM model, whereas for n uncertain parameters is $1 + m \times n + \binom{n}{2}$ [14].

The size and complexity of the approximation model for multiple input variables increase with the number of input variables and the order of polynomials. Therefore, the number of input variables and the order of polynomials must be relatively small to harness the advantages of the proposed method [17]. The accuracy of the approximation results depends on the selection of the most representative collocation points used to estimate the approximation model. The high-order of polynomials do not ensure more accurate approximations due to extremely uncertain features of these input parameters [22]. Thus, if the collocation points for the high-order polynomials lie from low probability regions (e.g., in Fig. 1, the probability density is low for normalized solar irradiance higher than 0.9), then the estimated values might affect the accuracy of the approximation.

4. Uncertainty assessment method for grid strength analysis

To evaluate the strength of the power system under uncertain renewable generation, the ESDSCR-based method is integrated with the PCM, which probabilistically models the impact of uncertain renewable generation based on their historical data and evaluates the probabilistic results instead of deterministic values.

4.1. Probabilistic model of renewable generation

The historical data unique to the installation site can demonstrate the uncertainty characteristic of renewable generation. In this paper, photovoltaic (PV) generation is considered as the uncertain parameter, which is a function of the PV irradiance. Thus, the effect of PV irradiance on grid strength is discussed and evaluated based on ESDSCR. The forecasted or the historical data for PV irradiance can be used for probabilistically modeling the uncertain nature of PV generation. The actual PV irradiance data from 2015 to 2020 was retrieved from the NREL database [23] to accurately represent the probability models of PV irradiance. Like in many studies [24], the variation of irradiance data is modeled as beta distribution. For example, in Fig. 1, the beta distribution is used to fit the histogram of the five year long raw data of PV irradiance at 12 pm. The shape parameters a and b from the beta distribution fit are obtained as 2.3318 and 2.1218, respectively, which are used to represent the irradiance distribution of solar PVs. Here, the probabilistic modeling of the input PV irradiance is treated as independent probability distributions. Eq. (11) represents the pdf for solar irradiance.

$$pdf(\xi) = \begin{cases} \frac{\Gamma(a+b)}{\Gamma(a)\Gamma(b)} \times \xi^{(a-1)}\times \\ (1-\xi)^{(b-1)}, & \text{for } 0 \le \xi \le 1, a \ge 0, b \ge 0 \\ 0, & \text{otherwise} \end{cases} \tag{11}$$

where ξ is solar irradiance in $\mathrm{kW/m^2}$, $\Gamma(.)$ is the Gamma function, and a and b are parameters of the beta pdf.

The power generated from a PV module depends on solar irradiance, ambient temperature, and the module characteristics [25]. The equations in (12) are used to find the power generated by the PV plant [26]. Note that the PV cell temperature is neglected.

$$P_{PV}(\xi) = \begin{cases} P_R\left(\frac{\xi^2}{\xi_{std}\xi_c}\right), & 0 < \xi < r_c \\ P_R\left(\frac{\xi}{\xi_{std}}\right), & \xi > r_c \end{cases} \tag{12}$$

where ξ_{std} is the solar irradiance in standard environment (1000 $\mathrm{W/m^2}$), ξ_c is the minimum solar irradiance (150 $\mathrm{W/m^2}$), and P_R is the rated output power of the PV farm.

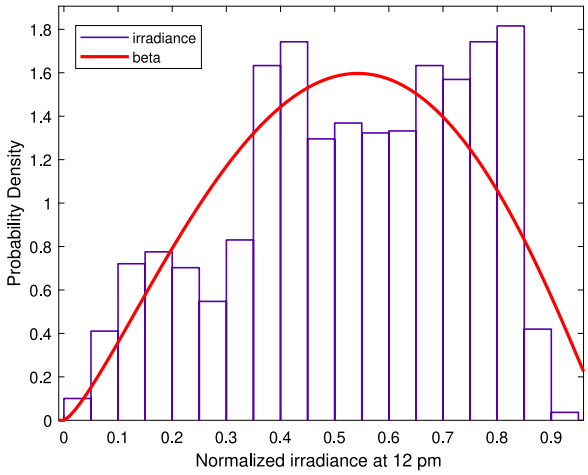

Fig. 1. Beta distribution fit for solar irradiance at 12 pm of NREL data [23].

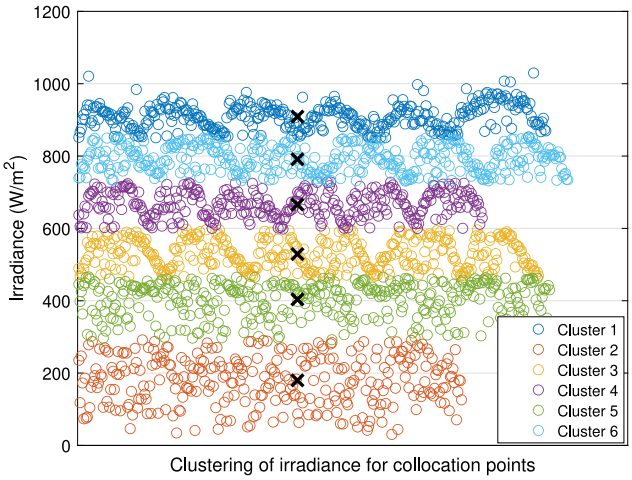

Fig. 2. Clusters of solar irradiance using k-means clustering method.

To derive the orthogonal polynomials of the PV irradiance for the application of the PCM, we consider Jacobi polynomial which is orthogonal over [−1,1] with respect to the weighting function $(1-x)^{\alpha}(1+x)^{\beta}$ with $\alpha > -1$ and $\beta > -1$.

$$\int_{-1}^{1} P_i(x)P_j(x)(1-x)^{\alpha}(1+x)^{\beta}dx = 0, \quad i \neq j \tag{13}$$

The weight function for Jacobi polynomials can be rearranged to represent the density function of a beta distribution. The orthogonal polynomials for the representative distribution can be derived by the method described in [27]. Eq. (13) can be rearranged by comparing it with the Jacobi polynomials and is written in terms of y as a transitional variable.

$$\int_{0}^{1} P_i(1-2y)P_j(1-2y)(y)^{\alpha}(1-y)^{\beta}dy = 0, \quad i \neq j \tag{14}$$

where $x = 1-2y$ and y is a random variable with the parameters for beta distribution as $\alpha+1$ and $\beta+1$.

Using (14) and the Gram–Schmidt process [21], the orthogonal polynomials for PV irradiance for the solar generators can be derived. These orthogonal polynomials are used to obtain the collocation points and to build the approximation model for grid strength in terms of PV irradiance.

4.2. K-means method for generating collocation points

Compared with MCS, PCM significantly reduces the total simulation burden since it requires fewer number of cases to determine the constant coefficients of the approximation model. However, the selected samples for the approximation model must be representative; otherwise, the approximation results could be inaccurate. The traditional PCM commonly uses the root method to select approximation samples by the combinations of the roots of the orthogonal polynomials [14,15].

To select samples that can fully describe the probabilistic characteristics, this paper use K-means clustering algorithm, which is a standard algorithm for reducing data dimensionality by representing the data with a smaller number of samples [18,28]. The K-means clustering method can split N number of data into k clusters based on data similarities. The objective of K-means clustering is to minimize the sum of the squared distances between the data and the centroid in each cluster and categorize all the data into N clusters. Mathematically, it minimizes the sum of Euclidean distances between each data point and the centroid in each cluster, which is written as,

$$\min \sum_{k=1}^{N_k} \sum_{i=1}^{n_k} \|\xi_i - c_k\|^2 \tag{15}$$

where ξ_i is the data point, c_k is the centroid of the kth cluster, N_k is the number of cluster, and $\|\xi_i - c_k\|$ is the Euclidean distance between ξ_i and c_k.

The main steps of K-means clustering are listed as follows:

1. Define the number of the clusters N_k.
2. Choose initial data points as cluster centroids c_k.
3. Compute the distances between data points and the centroid of each cluster.
4. Reassign the data point to the cluster with minimum distance to the cluster centroid.
5. Calculate the average of the data points of each cluster to obtain k new centroid location.
6. Repeat steps (3)–(5) until the cluster assignments do not change.

Fig. 2 shows the results of applying K-means clustering method to the NREL data shown in Fig. 1. It can be seen from Fig. 2 that the PV irradiance is divided into six clusters and each cluster centroid (denoted as **X**) is representative of the irradiance data of each cluster. The cluster centroids obtained are {179.83, 403.61, 528.95, 665.89, 791.15, 909.06} W/m^2, which can be used to determine the coefficients of the approximation model.

4.3. Uncertainty assessment method for grid strength analysis

Based on the ESDSCR-based method, the PCM method, and K-means clustering method, the uncertainty evaluation method for grid strength analysis is illustrated in Fig. 3. The main steps of the proposed is summarized below:

1. Obtain the actual historical/predicted data of uncertain input parameters such as solar irradiance or solar power generation and then convert them into intermediate variables using (13)–(14) to obtain appropriate pdf of uncertain parameters. Evaluate orthogonal polynomial functions from the obtained pdf based on Eqs. (4)–(6).
2. Develop the polynomial models for the ESDSCR with respect to uncertain input variables of corresponding solar irradiance in step (1) using (8) or (10) and unknown coefficients.
3. Compute the collocation points using k-means clustering method and run power flow calculation at these points to find the corresponding output response of the ESDSCR defined in (2).
4. Use these calculated collocation points and the corresponding output of ESDSCR in step (3) to obtain the unknown coefficients of the approximation model for ESDSCR developed in step (2) to assess grid strength based on the ESDSCR under uncertain solar generation.

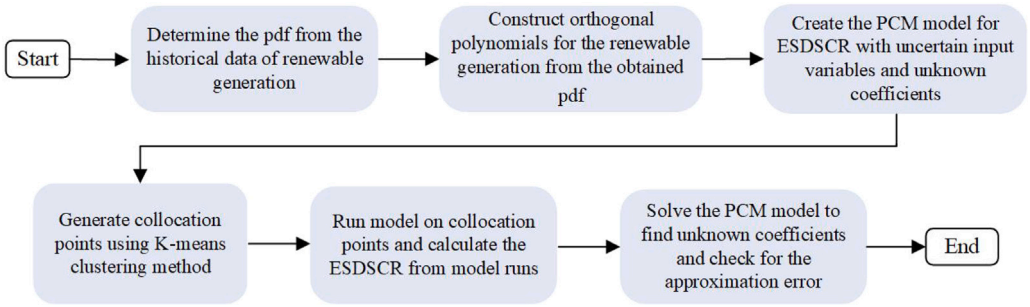

Fig. 3. Flowchart of the uncertainty evaluation method for grid strength analysis.

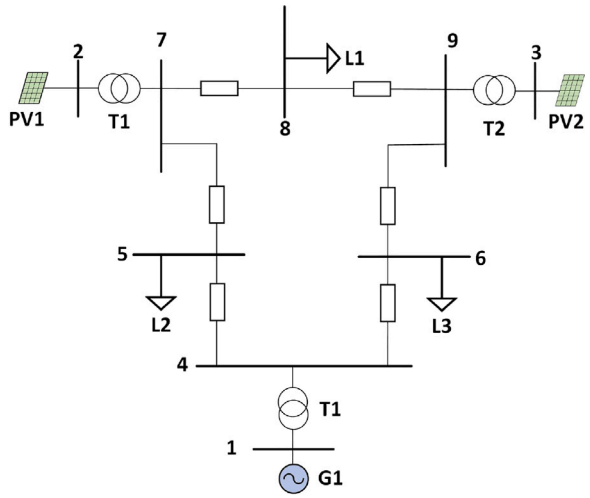

Fig. 4. Modified IEEE 9 bus system with two solar farms.

5. Case studies

5.1. System description

The proposed method for quantifying the impact of uncertain renewable generation on grid strength is validated on the modified IEEE 9-bus and IEEE 39-bus systems. In the modified IEEE 9-bus system as shown in Fig. 4, the two synchronous generators at buses 2 and 3 are replaced with two solar farms with 100 MW and 50 MW rated power, respectively. The values of the parameters for the beta pdf and the orthogonal polynomials for the respective irradiance of the solar farms are listed in Table 1, where $H_i(y_1)$ represents the orthogonal polynomials for solar farm 1 and $G_i(y_2)$ for solar farm 2. The roots from $H_i(y_1)$ and $G_i(y_2)$ is later converted back to relevant solar irradiance.

In the modified IEEE 39 bus system as shown in Fig. 5, the synchronous generators in different buses are replaced by solar farms. The beta distribution is used to fit the raw irradiance data for different time periods and the parameters obtained, as shown in Table 2, are used to define the pdf of irradiance for the solar farms. The beta distributed irradiance parameters $(\xi_1, \xi_2, \ldots, \xi_6)$ are rearranged using Jacobi polynomials (14) to find the orthogonal polynomials using the Gram–Schmidt process [21] and recursive formula described in [27]. The collocation points are determined using the k-means clustering method and used to find the coefficients of the $(1st - 3rd)$ orders approximation model for ESDSCR using (9). In the modified 9-bus and 39-bus system, the irradiance at a different time period (e.g. at 12 pm, 1 pm, etc.) from the Baseline Measurement System of the Solar Radiation Research Laboratory of NREL [23] are used in the solar farms as irradiance data for the diversity of irradiance in each farm.

To evaluate the accuracy of the approximation results, (MCS) results are used as a reference. The sum-squared-root error (e_{SSR}) is computed as an index for quantifying the accuracy of the PCM approximate model, and it is given by [16],

$$e_{SSR} = \sqrt{\frac{\sum_{i=1}^{\eta} (\hat{Y}_i - Y_i)^2 f(\vartheta_i)}{\eta f(\hat{\vartheta})}} \tag{16}$$

where Y_i is the actual output from the simulation run, $\hat{Y}_i$ is the estimated output, η is the collocation points, $f(\vartheta_i)$ is the joint pdf and $f(\vartheta)$ is the pdf of the highest probability collocation point. The relative sum-squared-root error (e_{RSSR}) can also be computed as normalized version [29],

$$e_{RSSR} = \frac{e_{SSR}}{\mu(\hat{Y})} \tag{17}$$

where $\mu(\hat{Y})$ is the mean value of $\hat{Y}$.

5.2. Comparison of K-means clustering method to traditional root method

The advantage of the K-means clustering method for collocation points selection over the root method is demonstrated on the modified IEEE 9-bus system. To show the advantage of the K-means clustering technique, the collocation points generated by K-means clustering method and the root method of these orthogonal polynomials [14,15] are compared with the results from MCS by 10,000 simulation runs.

In this comparison, the PCM approximation model for ESDSCR at buses 1 and 2 with different orders ($1st$–$3rd$ order) are derived using collocation points obtained from K-means clustering method and traditional root method and compared with MCS results. The approximation errors for each order of approximated model for both methods are calculated based on (16) and (17). Table 3 compares the errors, the mean value (μ), and the variance value (σ^2) of MCS method and three different orders of PCM approximate models for ESDSCR at bus 2 and 3 derived using collocation points obtained from K-means clustering method and traditional root method. Table 4 compares the computational times of the MCS method and different orders of the PCM approximation using collocation points obtained from K-means clustering method and traditional root method.

It can be observed from Table 3 and Figs. 6–7 that the K-means clustering method provides better collocation points of the PCM approximate models for ESDSCR at buses 2 and 3 than the traditional root method. As shown in Fig. 6, when the K-means clustering method is used to generate the collocation points, the 2nd approximate model is better than the other orders of the PCM approximate models for ESDSCR at bus 2; when the traditional root method is used to generate the collocation points, the 1st approximate model is better than the other high orders of the PCM approximate models. It can be observed from Table 3 that the approximation errors, the mean, and variance of the 2nd approximation model determined based on the K-means clustering method (i.e. e_{SSR}=1.1204, e_{RSSR}=0.2989, μ=3.7808 and σ^2=1.8801), are much closer to those of MCS results than those of the

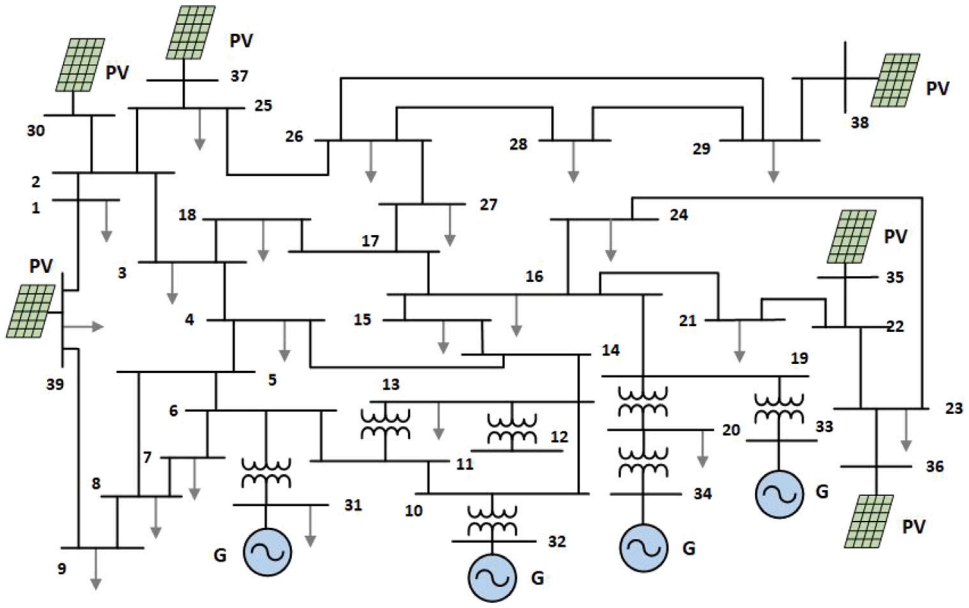

Fig. 5. Modified IEEE 39 bus system with six solar farms.

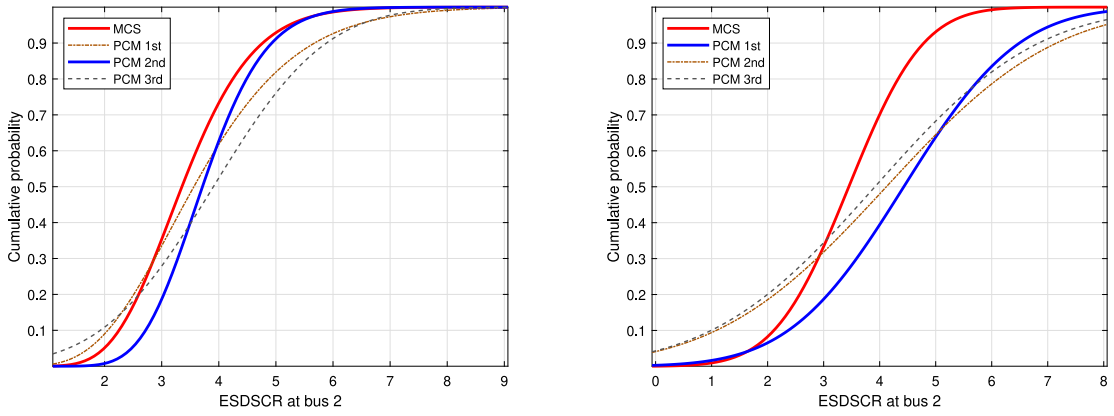

(a) Collocation points generated by K-means clustering method

(b) Collocation points generated by traditional root method

Fig. 6. Cumulative distribution plot of MCS and different orders of PCM approximate models for ESDSCR at bus 2 derived using collocation points obtained from K-means clustering method and traditional root method.

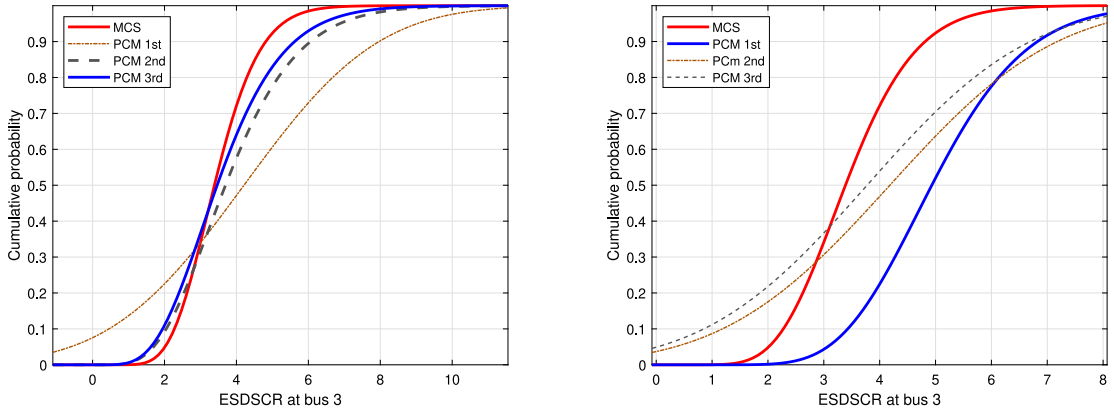

(a) Collocation points generated by K-means clustering method

(b) Collocation points generated by traditional root method

Fig. 7. Cumulative distribution plot of MCS and different orders of PCM approximate models for ESDSCR at bus 3 derived using collocation points obtained from K-means clustering method and traditional root method.

Table 1
Parameters and orthogonal polynomials for solar farms.

Solar farm 1 ($a = 2.33 \& b = 2.12$)
$H_1(y_1) = 2.225y_1 + 0.105$
$H_2(y_1) = 4.3940{y_1}^2 + 0.28612y_1 - 0.8007$
$H_3(y_1) = 8.4592{y_1}^3 + 0.6306{y_1}^2 - 3.3886y_1 - 0.1019$
$H_4(y_1) = 16.1893{y_1}^4 + 1.3013{y_1}^3 - 10.2355{y_1}^2 - 0.4775y_1 + 0.6835$
...
Solar farm 2 ($a = 2.12 \& b = 1.71$)
$G_1(y_2) = 1.915y_2 + 0.205$
$G_2(y_2) = 3.5198{y_2}^3 + 0.4950y_2 - 0.7077$
$G_3(y_2) = 6.4954{y_2}^3 + 1.0203{y_2}^2 - 2.7918y_2 - 0.1821$
$G_4(y_2) = 2.0883{y_2}^4 + 2.0167{y_2}^3 - 8.0735{y_2}^2 - 0.7969y_2 + 0.5790$
...

Table 2
Parameters for solar farms.

Bus		30	35	36	37	38	39
Rated power (MW)		250	650	560	540	830	1000
Parameters	a	2.33	2.07	2.01	1.74	2.12	2.14
	b	2.12	2.37	3.35	4.80	1.71	1.71

Table 3
Comparison of K-means clustering and traditional root methods for collocation point selection.

Bus	PCM	MCS		K-means clustering				Traditional root			
	order	μ	σ^2	μ	σ^2	e_{SSR}	e_{RSSR}	μ	σ^2	e_{SSR}	e_{RSSR}
	1			3.7476	1.9864	2.0328	0.5369	4.311	2.5921	**1.4852**	**0.233**
2	2	3.4492	1.9004	3.7808	1.8801	**1.1204**	**0.2989**	4.1196	5.6155	3.5225	0.9898
	3			3.9063	1.9676	1.3494	0.3454	3.9158	5.2074	3.2401	0.8274
	1			3.7459	3.5633	1.8204	0.4247	5.0513	1.582	**1.3685**	**0.2709**
3	2	3.4833	1.1109	3.6414	1.8314	1.5933	0.4047	4.2772	5.0636	3.4023	0.8688
	3			3.6646	1.7691	**1.1959**	**0.3281**	3.7756	5.2028	2.757	0.7302

Table 4
Computational time (s) for different methods.

PCM order	MCS	K-means clustering	Traditional root
1		0.69	1.88
2	102.71	1.09	2.11
3		2.5	2.89

1st approximation model determined by the traditional root method (i.e., e_{SSR}=1.4852 and e_{RSSR}=0.233, μ=4.3110 and σ^2=2.5921). Similar observation can be obtained from Fig. 7 and Table 3 for the PCM approximate models for ESDSCR at bus 3. Thus, the approximation model using K-means clustering method yields better selection of the collocation points to provide more accurate estimation when compared to using the traditional root method. In addition, it can be observed from Table 4 that while the PCM approximation model using either K-means clustering or traditional root method for collection point selection is more computational efficient than the MCS, the PCM approximation model using K-means clustering is slightly better that using the traditional root method regarding the computational efficiency.

5.3. Validation of the proposed method

5.3.1. PCM simulation in various orders

The ESDSCR values for all the solar PV buses are estimated using the proposed method and MCS. Table 5 presents the means and variances obtained from the ($1st-3rd$) orders PCM model and MCS. The errors for the approximation models are calculated using (16) and (17) for each estimation and are presented in Table 5. For illustration, the cdf plot and pdf plot for the ESDSCR estimation at buses 36 and 38, using three different approximation models and MCS are shown in Fig. 8(a) and Fig. 8(b), respectively. It can be observed from Fig. 8(a) that the 2nd order approximation model provides a better estimation of ESDSCR at bus 36 than the 1st or 3rd order PCM models with probabilistic values of solar generation. Moreover, Table 5 shows the means and variances of ESDSCR at bus 36 from the 2nd order PCM model (i.e., 1.68 and 1.93) are closer to those from MCS (i.e., 1.95 and 1.17) than those of the 1st or 3rd order PCM models. Besides the statistics, the errors for 2nd order approximation (i.e., e_{SSR}= 1.11 and e_{RSSR}= 0.55) are lower than those of the other orders. Thus, the 2nd order PCM approximation model provides a better estimation of ESDSCR at bus 36.

Likewise, Fig. 8(b) and Table 5 shows that the ESDSCR at bus 38 is better estimated using 1st order approximation than the higher order models. The means and variances of the 1st order PCM model (i.e. 1.4250 and 0.8721) are closer to the MCS results (i.e. 1.5875 and 1.7533) compared to the other higher order PCM models. The errors (i.e., e_{SSR}= 1.28 and e_{RSSR}= 0.21) are the lowest for the 1st order PCM model, which further proves accuracy in estimation. The means and variances for the approximation model of each bus that matches closest to that of MCS is highlighted in Table 5 to indicate the order of the PCM model that provides the most accurate results. Furthermore, it is well established that the proposed method for probabilistic grid strength assessment can save a substantial amount of simulation runs and computational time compared with traditional MCS. For example, it takes 7 sets of collocation points to model the 1st order PCM, 28 sets of points for the 2nd order PCM model, whereas it requires 10,000 simulation runs in MCS for approximating the probability distribution of ESDSCR at a bus with the same level of accuracy.

5.3.2. Estimating ESDSCR for different PV penetration

The proposed approach is used to analyze the effect of different levels of uncertainty in solar generation on grid strength. In this case study, ESDSCR is estimated using PCM-based approach for different solar power penetration with respect to total load power in the system. Fig. 9 shows all possible values of ESDSCR at bus 38 for different PV penetrations based on the 1st order approximation, and the statistical results are presented in Table 6.

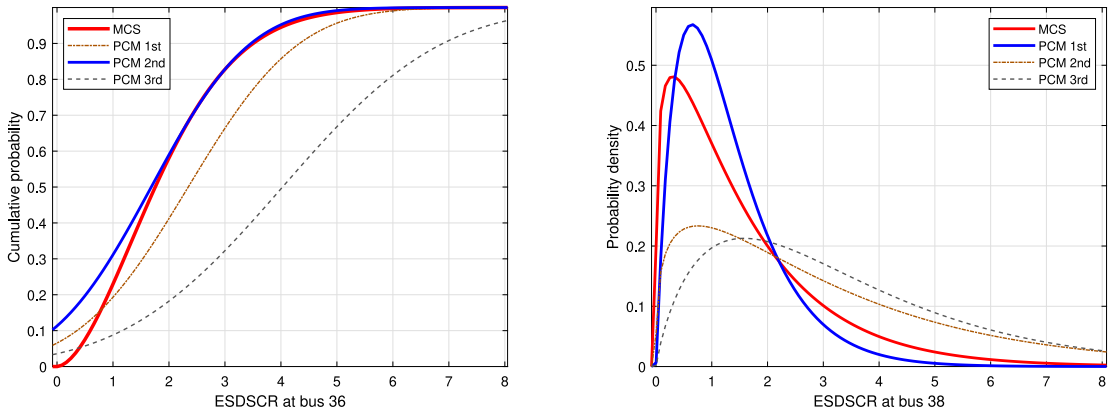

(a) Cumulative distribution plot of MCS and different order PCM approximate models of ESDSCR at bus 36

(b) Probability density plot of MCS and different order PCM approximate models of ESDSCR at bus 38

Fig. 8. Cumulative distribution plot of MCS and different orders of PCM approximate models of ESDSCR at buses 36 and 38.

Table 5
Statistic results of ESDSCR estimation using MCS and PCM for different PV buses.

PVBus	MCS		PCM 1				PCM 2				PCM 3			
	μ	σ^2	μ	σ^2	e_{SSR}	e_{RSSR}	μ	σ^2	e_{SSR}	e_{RSSR}	μ	σ^2	e_{SSR}	e_{RSSR}
30	2.0681	1.5312	**2.1071**	**1.6784**	2.02	0.94	3.9650	3.5580	5.28	1.33	1.8793	2.5212	3.61	1.92
35	2.0282	1.2307	**2.2734**	**2.7818**	2.63	1.16	2.9056	4.1963	3.07	0.77	3.4012	4.3138	4.03	1.17
36	1.9577	1.1788	2.3340	2.4068	1.31	0.65	**1.6838**	**1.9329**	1.11	0.55	4.0286	5.008	3.74	0.93
37	2.0276	1.6170	3.5284	4.2343	1.77	0.51	**2.7069**	**4.8220**	1.52	0.56	3.6152	5.261	2.99	0.82
38	1.5875	1.7533	**1.4250**	**0.8721**	1.28	0.21	2.4591	4.921	1.89	0.59	3.4240	3.8610	2.68	0.78
39	1.5794	1.7632	**2.7862**	**1.0382**	1.81	0.65	2.885	3.7702	1.37	0.44	2.9473	3.4564	2.41	0.82

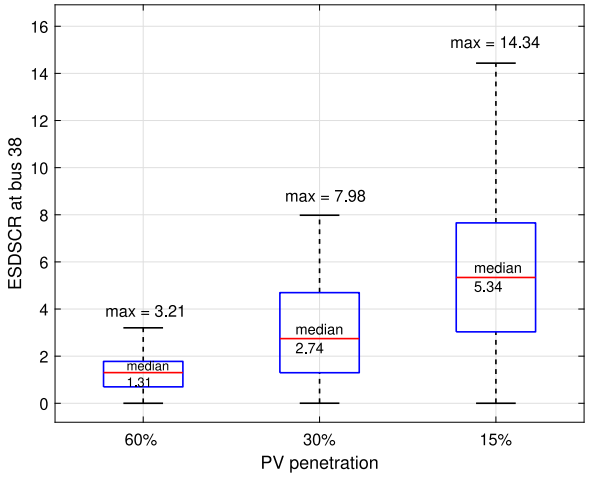

Fig. 9. Boxplot for ESDSCR estimation at bus 38 with different PV penetrations using 1st order approximation.

Table 6
Statistic results of ESDSCR estimation with different PV penetration.

PV penetration	60%	30%	15%
μ	1.4250	3.1132	5.4869
σ^2	0.8721	2.1013	3.1678

From Fig. 9 and Table 6, it can be seen that the increasing penetration of uncertain solar power leads to lower ESDSCR values and thus affects the grid strength. For higher PV power penetration (i.e., 60% penetration), the median of possible ESDSCR values lies at 1.31, which reflects that the grid tends to be very weak as $ESDSCR < 2$. For 30% PV penetration, the median of the ESDSCR values lies at 2.74 which shows that the grid tends to be weak as substantially ESDSCR lies between 2 and 3, and for 15% penetration, the median of ESDSCR values lies at 5.34, indicating mostly strong grid as $ESDSCR > 3$. This demonstrates that the risk of weak grid conditions increases with the higher penetration of solar generation. In Table 6, it can be seen that means and variances for uncertain ESDSCR for 60% PV penetration are lower, indicating a weak grid but for 15% PV penetration means and variances are higher, demonstrating strong grid conditions. This also verifies that grid strength tends to be weaker with higher PV penetration. This approach estimated grid strength for multiple uncertainty levels without a massive simulation burden and furnished quick visibility to system alteration. Thus, this proposed approximation method serves as a great visualization tool that can quantify the impact on grid strength due to uncertain renewable generation and instantaneously inform the power system planners of possible impacts.

6. Conclusion

This paper presented an approach to analyze the impact of uncertain renewable generation on grid strength by integrating the PCM with the ESDSCR-based method. In the proposed approach, the ESDSCR-based method was used for grid strength assessment, while the PCM was used to establish the approximation polynomial functions with multiple input variables for modeling the impact of uncertain renewable generation. To improve the approximation accuracy of the PCM, K-means clustering technique was applied in the selection of the approximation samples. The efficacy of the proposed approach is demonstrated on the modified IEEE 9-bus system and IEEE 39-bus system with multiple renewable resources. The proposed approach can save a massive number of simulation burden without compromising the accuracy of the approximation results compared to traditional Monte Carlo simulation. The proposed approach is promising for grid strength assessment under variable renewable generation to guide grid planning and operation for

identifying potential weak grid issues. In our future research, we will implement the proposed method in realistic renewable energy systems and extend the proposed method for grid strength assessment while considering inverter dynamics under uncertain renewable generation.

CRediT authorship contribution statement

Manisha Maharjan: Methodology, Software, Visualization, Investigation, Validation, Writing – original draft. **Almir Ekic:** Data curation, Software. **Mari Beedle:** Writing – review & editing. **Jin Tan:** Writing – review & editing. **Di Wu:** Conceptualization, Supervision, Writing – review & editing.

Declaration of competing interest

The authors declare that they have no known competing financial interests or personal relationships that could have appeared to influence the work reported in this paper.

Data availability

Data will be made available on request.

Acknowledgment

The authors would like to thank Emily L Barrett from PNNL for her valuable suggestions on the manuscript. The authors express their gratitude to the funding provided to support this study from National Science Foundation (NSF), USA EPSCoR RII Track-4 Program under the grant number OIA2033355. The findings and opinions expressed in this article are those of the authors only and do not necessarily reflect the views of the sponsors.

References

[1] NERC. Integrating Inverter-Based Resources into Low Short Circuit Strength Systems. Reliability Guideline. 2017, https://www.nerc.com/comm/PC_Reliability_Guidelines_DL/Item_4a._Integrating%20_Inverter-Based_Resources_into_Low_Short_Circuit_Strength_Systems_-_2017-11-08-FINAL.pdf.

[2] Ding Y, Singh C, Goel L, Østergaard J, Wang P. Short-term and medium-term reliability evaluation for power systems with high penetration of wind power. IEEE Trans Sustain Energy 2014;5(3):896–906.

[3] NERC. NERC essential reliability services task force: measures framework report. GA, USA: NERC Atlanta; 2015, http://www.nerc.com/comm/Other/essntlrlbltysrvcstskfrcDL/ERSTF%20Framework%20Report%20-%20Final.pdf.

[4] Zhang Y, Huang S-HF, Schmall J, Conto J, Billo J, Rehman E. Evaluating system strength for large-scale wind plant integration. In: 2014 IEEE PES general meeting| conference & exposition. IEEE; 2014, p. 1–5.

[5] Energy G. Minnesota renewable energy integration and transmission study. Minnesota Utilities & Transmission Companies and Minnesota Department of; 2014.

[6] Wu D, Li G, Javadi M, Malyscheff AM, Hong M, Jiang JN. Assessing impact of renewable energy integration on system strength using site-dependent short circuit ratio. IEEE Trans Sustain Energy 2017;9(3):1072–80.

[7] Sanni SO, Akorede MF, Olarinoye GA. Strength assessment of electric power systems containing inverter-based distributed generation. Electr Power Syst Res 2022;207:107825.

[8] Zhang F, Xin H, Wu D, Wang Z, Gan D. Assessing strength of multi-infeed LCC-HVDC systems using generalized short-circuit ratio. IEEE Trans Power Syst 2018;34(1):467–80.

[9] Xiao H, Zhang Y, Duan X, Li Y. Evaluating strength of hybrid multi-infeed HVDC systems for planning studies using hybrid multi-infeed interactive effective short-circuit ratio. IEEE Trans Power Deliv 2020;36(4):2129–44.

[10] Ekic A, Strombeck B, Wu D, Ji G. Assessment of grid strength considering interactions between inverter-based resources and shunt capacitors. In: 2020 IEEE power & energy society general meeting. IEEE; 2020, p. 1–5.

[11] Billiton R, Li W. Reliability assessment of electric power systems using Monte Carlo methods. New York: Spring; 1994.

[12] Krishayya P, Adapa R, Holm M, et al. IEEE guide for planning DC links terminating at AC locations having low short-circuit capacities, Part I: AC/DC system interaction phenomena. France: CIGRE; 1997.

[13] Zhang J, Tse C, Wang K, Chung C. Voltage stability analysis considering the uncertainties of dynamic load parameters. IET Gener Transm Distrib 2009;3(10):941–8.

[14] Hockenberry JR, Lesieutre BC. Evaluation of uncertainty in dynamic simulations of power system models: The probabilistic collocation method. IEEE Trans Power Syst 2004;19(3):1483–91.

[15] Webster MD, Tatang MA, McRae GJ. Application of the probabilistic collocation method for an uncertainty analysis of a simple ocean model. MIT Joint Program on the Science and Policy of Global Change; 1996.

[16] Zheng C, Kezunovic M. Impact of wind generation uncertainty on power system small disturbance voltage stability: A PCM-based approach. Electr Power Syst Res 2012;84(1):10–9.

[17] Preece R, Woolley NC, Milanović JV. The probabilistic collocation method for power-system damping and voltage collapse studies in the presence of uncertainties. IEEE Trans Power Syst 2012;28(3):2253–62.

[18] Fan M, Li Z, Ding T, Huang L, Dong F, Ren Z, et al. Uncertainty evaluation algorithm in power system dynamic analysis with correlated renewable energy sources. IEEE Trans Power Syst 2021.

[19] Australian Energy Market Operator. System strength in the NEM explained. AEMO Information & Support Hub; 2020.

[20] Liu Y, Chen Z. A flexible power control method of VSC-HVDC link for the enhancement of effective short-circuit ratio in a hybrid multi-infeed HVDC system. IEEE Trans Power Syst 2012;28(2):1568–81.

[21] Davis PJ, Rabinowitz P. Methods of numerical integration. Courier Corporation; 2007.

[22] Yin H, Zivanovic R. Using probabilistic collocation method for neighbouring wind farms modelling and power flow computation of South Australia grid. IET Gener Transm Distrib 2017;11(14):3568–75.

[23] NREL solar radiation research laboratory. 2021, http://www.blowinglotsofweirdstuffup.com/guide.html. (Accessed 18 December 2021).

[24] Hasan KN, Preece R, Milanović JV. Existing approaches and trends in uncertainty modelling and probabilistic stability analysis of power systems with renewable generation. Renew Sustain Energy Rev 2019;101:168–80.

[25] Pierrou G, Wang X. The effect of the uncertainty of load and renewable generation on the dynamic voltage stability margin. In: 2019 IEEE PES innovative smart grid technologies Europe. IEEE; 2019, p. 1–5.

[26] Surender Reddy S, Bijwe PR, Abhyankar AR. Real-time economic dispatch considering renewable power generation variability and uncertainty over scheduling period. IEEE Syst J 2015;9(4):1440–51.

[27] Gautschi W. Orthogonal polynomials (in matlab). J Comput Appl Math 2005;178(1–2):215–34.

[28] Chenxu W, Fei T, Hongsheng Z, Yixi Z, Chang L, Feifei W. An improved cumulant method for probabilistic load flow calculation. In: 2019 IEEE power & energy society general meeting. IEEE; 2019, p. 1–5.

[29] Chen W, Xie X, Wang D, Liu H, Liu H. Probabilistic stability analysis of subsynchronous resonance for series-compensated DFIG-based wind farms. IEEE Trans Sustain Energy 2017;9(1):400–9.